Effects of turbulence at the ingress into landfill gas wells

Abhishek Baral, Mehrdad Sepehri and Yana Nec
Department of Mathematics and Statistics
Thompson Rivers University, British Columbia, Canada

Abstract
Landfill gas collection underpins environmental protection and energy recovery in solid waste management. The objective of this study is to incorporate turbulence at the interface between the porous landfill mass and unobstructed pipe flow, and test the impact on operation efficiency of landfill gas wells. Darcy flow in the porous media is coupled with Reynolds-averaged Navier-Stokes equations within the well subject to two turbulence closure models. A significant discrepancy in head losses within the well and across the landfill is observed between the result of that approach and past studies, where the coupling between the two types of flow was performed semi-analytically without addressing local flow structures at the well apertures. Strong localised pressure variation dominates the flow at the interface, inducing inner boundary layer type phenomena. The cumulative ingress impact diminishes the suction strength required for adequate gas extraction as well as pinpoints the vicinity of the intake apertures as the salient locus of head loss in the landfill mass, in stark contrast to the semi-analytical solution that employed quasi-1D geometry. The study conclusively proves the importance of accounting for turbulence at the ingress for a realistic representation of flow in landfill collection systems.

Keywords porous medium flow, Darcy's law, turbulence, RANS equations, landfill gas, collection well, collection efficiency

1 Background

Landfills are complex man-made facilities that require comprehensive engineering insight to operate safely and effectively. Multiple interdependent types of flows are associated with the various components of the landfill system. The difficulty to obtain a realistic faithful description of the composite fluid flow stems from the disparity of physical and mathematical laws governing each type of flow, and their coupling. The landfill mass is the main and most often the largest part of the system. Within it fluid moves through a solid matrix, whereby porous medium flow descriptions apply, with the prevalent momentum transfer mechanism being Darcy's law due to the low velocities observed. This is encountered in solutions in reduced symmetric settings (Wise and Townsend, 2011) through semi-analytical models with few input parameters (Nec and Huculak, 2017, 2019) and to numerical simulations with an extensive parameter space (Feng et al., 2015). Treatment of leachate requires multi-phase flow theory and studies thereof usually focus the attention on the processes occurring within the landfill mass alone (Hu et al., 2020; Lu et al., 2021; Ke et al., 2021).

Although formally the atmosphere is not a part of the landfill, in reality it interacts closely with the landfill cavity via barometric pressure and wind velocity fluctuations. By continuity these propagate through the partly permeable cover, affecting the pressure distribution within the landfill as well as the efflux of landfill gas and influx of air across the surface. Some studies perform only a one-sided analysis of fluid traversing the top boundary – from the landfill out, with the purpose to determine the lateral zone of influence (Nec and Huculak, 2019; Halvorsen et al., 2019). The full

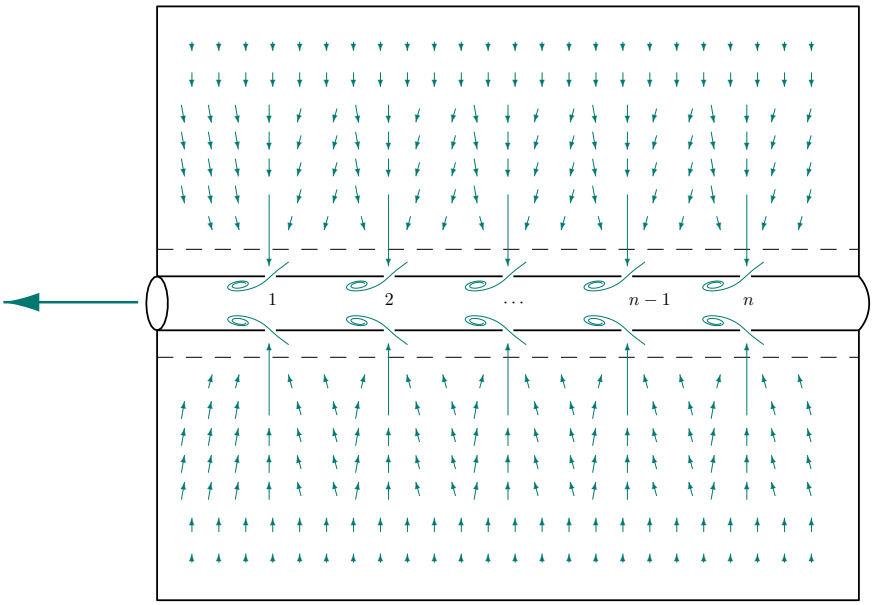

Figure 1: Landfill and well flow schematic: well pipe supported by a gravel lamina (dashed lines) and imbedded within a gas generating waste layer; perforated sections numbered from outlet; general flow directions (arrows), regions of acceleration (varying arrow length) and turbulent mixing (spirals); dimensions not to scale.

framework requires a turbulent atmospheric flow description coupled to the porous medium flow through the landfill cover (Rees-White et al., 2019).

Imbedded either vertically or horizontally within the waste mass is a network of perforated collection pipes. In the pipes the fluid motion is governed by the continuity and momentum equations of unobstructed continuum flow. The complication lies in coupling it correctly to the flow in the surrounding porous matrix. The smallest, yet crucial component of the system is a set of ingress apertures into the pipes, where the flow might be thought of as a reversed jet. It will be shown hereunder that the extraction energy depends closely on an accurate modelling of the ingress flow, impacting the collection system efficiency and economic viability of the usage of landfill gas as a renewable energy source. The disparity of the smaller characteristic dimensions (pipe and ingress aperture radii) relative to the overall system dimensions (landfill radius and pipe length) is extreme: the ratio of aperture radius to pipe length is $\mathcal{O}\left(10^{-5}\right)$. This circumstance renders tridimensional numerical simulations exceedingly costly and has historically hindered the development of computational fluid dynamics simulations for this application. Quite counter-intuitively the coupling of two distinct types of flow has so far defied mathematical tools such as conventional asymptotic theory usually brought to bear in systems with so well defined scale separation, whilst analytical and semi-analytical approaches in one-dimensional or quasi-one-dimensional geometry misrepresented the pressure distribution in the system. To the best of the authors' knowledge, this is the first study analysing a landfill gas flow field with full ingress turbulence and mixing in the collection well.

In order to isolate the effect of turbulence at the interface, where the Darcy and continuum flows are coupled, a simple axisymmetric geometry is chosen with a sealed boundary. A schematic is

shown in figure 1: the gas generated as part of the waste degradation process traverses two porous layers – waste and gravel, and then enters the well through apertures, where substantial turbulent effects are expected, as can be inferred from comparison of the flow geometry and resultant stream mixing with such systems as jet injection (Broadwell and Breidenthal, 1984) as well as empirical pipe juncture models (Idel'chik, 1966).

A semi-analytical solution for a horizontal well was developed previously, employing a simplistic mixing mechanism upholding conservation of mass and continuity of pressure at the interface between the porous medium and pipe flow, but not taking turbulence into account in the vicinity thereof (Nec and Huculak, 2019). The flow within the pipe was modelled via the classical Darcy-Weisbach turbulence description modified for a weakly compressible fluid (Nec and Huculak, 2017). The inflow into the well is similar in nature to the jet systems, whose behaviour has been extensively studied without arriving at one widely accepted perspective, a testament to the complexity of flow structures underlying the process of mixing and alignment of two fluid streams. The flow field around a well aperture is at least as complicated as near a jet injection site: there is no control of fluid entry angle relative to the pipe wall, and the momentum equations change dramatically when the fluid transitions from a porous medium to continuum flow. In light of the above, the objectives of this study are to simulate the flow of gas as it travels through two porous media and into the well, examine the limitations of the semi-analytical solution and gain qualitative insight into the flow regime at the ingress to the well with the view to improve the design and efficiency of operation of horizontal collection wells.

2 Geometry and governing equations

The model comprises a cylindrical well surrounded by two porous annuli. The axial symmetry is essential to attain both the exact solution underpinning the quasi-1D reduction described in §2.1, and reasonable computation time in the fully turbulent model given in §2.2. To this end the perforations were simplified to slits of an equivalent area. In order to replace n_h circular holes of radius r_h (small relative to the pipe radius r_p), the width δ of the required slit must be

$$\delta = n_h \frac{{r_h}^2}{2r_p}. \tag{1}$$

In the horizontal well the axisymmetric apertures might also represent a situation, where the well is constructed of loosely overlapping telescopic pipe segments with no additional perforations. Figure 2 gives a schematic of the solution domain. The fully turbulent numerical model and the semi-analytical reduction share the following boundary conditions: prescribed constant pressure at the well outlet; zero normal flux on the landfill perimeter and well end plane; continuity of pressure and velocity on the contiguity surface between the two porous annuli. In the numerical model the normal flux on the outlet plane and pipe wall contiguous to the gravel lamina, as well as velocity on all surfaces of the pipe in contact with the continuum flow are set to vanish. When the quasi-one-dimensional reduction is performed in the semi-analytical model, these surfaces conceptually cease to exist. The replacement conditions are discussed in §2.1. A requirement of continuous pressure and velocity on the perimeter of all slits couples the porous medium and continuum flows.

The flow within the porous matrix is not expected to be turbulent due to the very low velocity and thus Reynolds number in that part of the system, identically for both the numerical and semi-analytical models. Within the landfill the momentum transfer is governed by Darcy's law (Whitaker, 1986)

$$\mathbf{u} = -\frac{k_{\text{eff}}}{\mu}(\nabla p + \rho \mathbf{g}), \tag{2a}$$

wherein $\mathbf{u}$ is the velocity field resulting when a motion of fluid of density ρ and dynamic viscosity μ through a medium of permeability k_{eff} is induced by pressure gradient ∇p and gravity field $\mathbf{g}$. Gravity

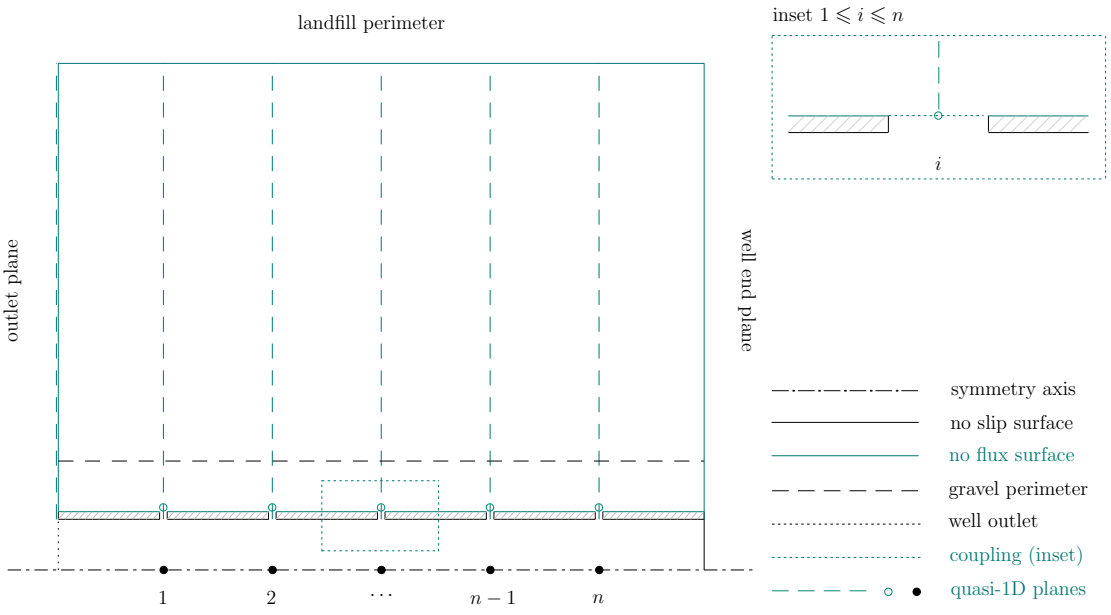

Figure 2: Boundary and coupling conditions: axial symmetry at well centre line (dash-dotted); no slip on inner pipe walls as well as aperture walls (solid black enclosing hatched pipe segments); no flux on landfill perimeter, outlet and well end planes, and outer pipe walls (solid green / grey); continuity of pressure and velocity on waste-gravel contiguity perimeter (dashed black); constant pressure at well outlet (dotted black); continuity of pressure and velocity on porous medium - continuum flow coupling interface (dotted green / grey, inset); matching pressure immediately outside and in the well (clear / full circles) on quasi-1D collection of planes (green / grey dashed lines).

is essential if the well is vertical, but might be neglected in horizontal wells, whose main head loss mechanism is friction. The permeability k_{eff} is assigned distinct effective values for waste and gravel layers. In the earlier days of the development of porous medium flow theory the permeability as the measure of resistance to fluid flow was deemed an attribute of the solid matrix alone, particularly the geometry of the packing particles (Carman, 1937). In time it was understood that the interaction of a specific fluid-matrix pair was quite complex, leading to numerous generalisations of the original Kozeny-Carman equation via a variety of approaches from probability distributions (Panda and Lake, 1994) to fractals (Henderson et al., 2010). In a landfill system the issue is further exacerbated by the irregularity in packing particles' shape and size. An effective value is taken to represent a reasonable order of magnitude based on data and experience accumulated by industry professionals when adjusting suction strength to ensure slightly sub-atmospheric pressure throughout the system. At steady state the conservation of mass is identical to that of continuum flow (Fulks et al., 1971)

$$\nabla \cdot (\rho \mathbf{u}) = C, \tag{2b}$$

where the generation rate C is taken constant and spatially uniform in the waste layer, and vanishing in the gravel. The thermodynamic conditions in the landfill are of moderate temperatures and pressures, whereby the assumption of ideal gas is well tenable. Hence

$$p = \rho R T, \tag{2c}$$

with R standing for the gas constant and T – temperature, both taken as effective constant values.

The governing equations for the unobstructed flow within the well and the coupling to the Darcy flow (2) differ between the two models. The semi-analytical reduction employs the classical empirical modelling based on data for turbulent pipe flows (Colebrook, 1939). The coupling is performed by using the pressure in the well as a boundary value for the profile in the porous medium at a discrete set of points aligned with the perforated sections (circle marks in figure 2). Further detail is given in §2.1. The full numerical model solves Reynolds-averaged Navier-Stokes equations subject to $k-\epsilon$ and $k-\omega$ turbulence closure methods, as detailed in §2.2. The coupling is done via a continuity of pressure at the interface between the porous media and free flow (see inset of figure 2). The continuity of velocity follows automatically, since the mass conservation obeys the homogeneous version of equation (2b) identically on both sides of the interface.

2.1 Quasi-one-dimensional semi-analytical model

Substituting (2a) and ρ obtained from (2c) into (2b) yields a differential equation for p alone. In the steady one-dimensional axisymmetric case its solution for the pressure at distance r from the well centre is given by

$$p = \sqrt{-\frac{\mu}{2k_{\text{eff}}} RTCr^2 + a\ln r + b}\,, \tag{3}$$

with a and b integration constants, distinct for each porous lamina and determined from boundary conditions (Nec and Huculak, 2019). The quasi-1D model is underpinned by an assumption of slow longitudinal variation throughout, and coupling of porous medium and pipe flows as follows. Set the origin $(r,\ell)=(0,0)$ at the centre of the pipe within the outlet plane. The perforated sections are located at points ℓ_i, $i=\{1,\ldots,n\}$, numbered from the outlet. The pipe segments are numbered respectively, so that segment i is delimited by $[\ell_{i-1},\ \ell_i]$ with $\ell_0=0$ corresponding to the outlet. Denote the mass flowrate within segment i by $\dot{m}_i$. Conservation of mass must hold at each perforated section. If $\Delta\dot{m}_i$ is the flowrate incoming at section i, then

$$\dot{m}_{i-1} = \dot{m}_i + \Delta\dot{m}_{i-1}, \quad i=\{2,\ldots,n\}. \tag{4a}$$

Integration constants in (3) are chosen so that the pressure inside and outside of the well (circle marks in figure 2) equals:

$$p\left(r_p^+,\ell_i\right) = p\left(r_p^-,\ell_i\right), \quad i=\{1,\ldots,n\}, \tag{4b}$$

where $p\left(r_p^+,\ell_i\right)$ is the pressure at aperture in position ℓ_i as given by the porous medium flow and $p\left(r_p^-,\ell_i\right)$ is the pressure at the same point as given by the unobstructed pipe flow. Within the last blocked segment of the pipe $\dot{m}_n=0$, and thus

$$\dot{m}_{n-1} = \Delta\dot{m}_{n-1} \tag{4c}$$

must hold. This condition acts as the convergence criterion. The pressure variation within any one segment of the well is given by a non-linear relation that depends on the prevalent head loss mechanism: friction, gravity or both (Nec and Huculak, 2017). With friction only (horizontal well) $p\left(r_p^-,\ell_i\right)$ and $p\left(r_p^-,\ell_{i+1}\right)$ are related via

$$\frac{4r_p}{f}\ln\frac{p\big|_{\ell_i}}{p\big|_{\ell_{i+1}}} - \frac{2\pi^2 r_p^5}{f\dot{m}_i RT}\left(p^2\Big|_{\ell_i} - p^2\Big|_{\ell_{i+1}}\right) = \ell_{i+1}-\ell_i, \tag{5a}$$

where f is the friction coefficient as given by the Colebrook equation (Colebrook, 1939; White, 1999)

$$\frac{1}{\sqrt{f}} = -2\log_{10}\left(\frac{\varepsilon}{3.7} + \frac{2.51}{\mathrm{Re}\sqrt{f}}\right) \tag{5b}$$

that requires the Reynolds number Re and relative pipe wall roughness ε (both diameter based) as input. Equation (5b) stems from an empirical fit of large sets of data reported for turbulent flow in smooth as well as rough pipes. In simple pipe flow the division into laminar, transient and turbulent flow regimes is based on the Reynolds number. In the landfill well Re ranges from zero at the blocked end to values on the order of $\mathcal{O}\left(10^4\right)$ at the outlet. Due to the abrupt change of flow direction at the ingress and mixing of the incoming fluid with the crossflow within the well, the flow is expected to be turbulent even at the last few segments of the well, where the nominal Re might be relatively low. Thus equation (5b) applies for all $1 \leqslant i \leqslant n$.

With gravity only (vertical well) the relation between $p\left(r_p^-, \ell_i\right)$ and $p\left(r_p^-, \ell_{i+1}\right)$ is

$$\ln \frac{p\big|_{\ell_i}}{p\big|_{\ell_{i+1}}} + \frac{\dot{m}_i^2 RT}{2\pi^2 r_p^4}\left(\frac{1}{p^2\Big|_{\ell_i}} - \frac{1}{p^2\Big|_{\ell_{i+1}}}\right) = \frac{g}{RT}\left(\ell_{i+1} - \ell_i\right), \tag{5c}$$

where g is the constant of gravity. In either case the problem is solved iteratively until convergence to a desired accuracy.

The quasi-1D representation of the landfill is equivalent to a sequence of thin generating discs aligned with the slits and satisfying system (4). Whilst this construction is useful when seeking a reasonable estimate of the well functionality owing to its quick convergence and easy implementation in freely available software (Octave, 2020), a finer optimisation of the flow field is impossible, since any variation between the discs or the mixing structures in the vicinity of ingress apertures are inaccessible.

2.2 Two-dimensional numerical model

The velocities away from the pipe are known to be very low, as is the local Reynolds number, whether based on the characteristic pore length scale or one of the global dimensions of the landfill. However, the acceleration near the well apertures is tremendous, resulting in velocities higher by several orders of magnitude relative to the core of the waste layer. This circumstance undermines the quasi-one-dimensional nature of the semi-analytical formulation with its asymptotically slow longitudinal variation throughout. Therefore the flow in the immediate vicinity of the apertures must be modelled as turbulent. Moreover, the flow upon ingress into the pipe must also be turbulent due to mixing of the incoming streams with the longitudinally flowing main stream, even if the nominal crossflow Reynolds number is not high, for instance near the blocked end of the well.

COMSOL Multiphysics simulation software (COMSOL, 2021) was used to couple Darcy's law in the porous media with Reynolds-averaged Navier-Stokes equations within the well, using the $k-\epsilon$ and $k-\omega$ turbulence closure models. The linearity of the mass continuity equation implies that its turbulent version for the averaged velocity vector $\mathbf{u}$ remains unchanged:

$$\nabla \cdot (\rho \mathbf{u}) = 0, \tag{6a}$$

with the dependence $\rho(p)$ set by (2c). Due to the non-linearity of the momentum equations, the averaging procedure introduces additional terms known as the Reynolds stress tensor:

$$\rho\,(\mathbf{u}\cdot\nabla)\mathbf{u} = \nabla\cdot(-p\mathbf{I} + \mathbf{K}), \tag{6b}$$

$$\mathbf{K} = (\mu + \mu_\mathrm{t})\left(\nabla\mathbf{u} + (\nabla\mathbf{u})^\mathrm{T} - \frac{2}{3}(\nabla\cdot\mathbf{u})\mathbf{I}\right) - \frac{2}{3}\rho k\mathbf{I}, \tag{6c}$$

where $\mathbf{I}$ is the identity matrix. With the $k-\epsilon$ closure method the coupled transport equations for the turbulent kinetic energy k and dissipation rate ϵ read

$$\rho\,(\mathbf{u}\cdot\nabla)k = \nabla\cdot\left[\left(\mu + \frac{\mu_\mathrm{t}}{\sigma_k}\right)\nabla k\right] + P_k - \rho\,\epsilon, \tag{7a}$$

$$\rho\,(\mathbf{u}\cdot\nabla)\epsilon = \nabla\cdot\left[\left(\mu+\frac{\mu_\mathrm{t}}{\sigma_\epsilon}\right)\nabla\epsilon\right] + c_{\epsilon_1}P_k\frac{\epsilon}{k} - c_{\epsilon_2}\rho\frac{\epsilon^2}{k}, \tag{7b}$$

where μ_t is the eddy viscosity

$$\mu_\mathrm{t} = \rho\,c_\mu\frac{k^2}{\epsilon} \tag{7c}$$

and

$$P_k = \mu_\mathrm{t}\left(\nabla\mathbf{u}:\left(\nabla\mathbf{u}+(\nabla\mathbf{u})^\mathrm{T}\right) - \frac{2}{3}(\nabla\cdot\mathbf{u})^2\right) - \frac{2}{3}\rho k\,(\nabla\cdot\mathbf{u}), \tag{7d}$$

with all remaining symbols standing for model constants: $\sigma_k = 1$, $\sigma_\epsilon = 1.3$, $c_{\epsilon_1} = 1.44$, $c_{\epsilon_2} = 1.92$ and $c_\mu = 0.09$ (COMSOL, 2021, §3, pp 207–215). With the $k-\omega$ closure system (7) is replaced by

$$\rho\,(\mathbf{u}\cdot\nabla)k = \nabla\cdot\left[\left(\mu+\frac{\mu_\mathrm{t}}{2}\right)\nabla k\right] + P_k - \beta^*\rho\,\omega\,k, \tag{8a}$$

$$\rho\,(\mathbf{u}\cdot\nabla)\,\omega = \nabla\cdot\left[\left(\mu+\frac{\mu_\mathrm{t}}{2}\right)\nabla\omega\right] + \alpha P_k\frac{\omega}{k} - \beta\rho\,\omega^2, \tag{8b}$$

where

$$\mu_\mathrm{t} = \rho\frac{k}{\omega} \tag{8c}$$

and P_k is given by (7d). The parameter α is constant, whereas β and β^* depend on both the mean vorticity and strain tensors, as well as k and ω, forming the revised Wilcox model. For complete detail the reader is referred to the COMSOL manual (COMSOL, 2021, §3, pp 215–220). The pressure resulting by (7) or (8) on the interface with the porous domain was used as a boundary condition for the Darcy flow in the landfill.

The ensuing coupled flow solution was compared to the semi-analytical prediction for a wide range of physical parameters, in particular several orders of magnitude of landfill media permeabilities and generation rates. The sole control parameter available to the operators – the well outlet suction – was modified to maintain slightly sub-atmospheric conditions throughout the system, as required by environmental regulations. Table 1 lists the geometric and physical parameter values common to all results, except where explicitly indicated.

2.3 Numerical model validation

The bulk of the results presented in §3 concerns the basic well comprising n segments with slit width δ. In §4 two double intake area configurations $(2\delta, n)$ and $(\delta, 2n)$ were considered. For each one the numerical solution was performed on a base mesh and validated on a fine mesh. Table 2 summarises the characteristics of each mesh used. The extreme disparity of geometric length scales of the computational domain requires caution when constructing the mesh: the ratio of the smallest dimension δ as given by (1) and the well length L is of the order $\mathcal{O}\left(10^{-6}\right)$. The implication thereof is twofold: mesh refinement was mainly focussed on the vicinity of the acceleration zone near the slit, as is attested by the significant increase of the number of elements in that region; the total number of elements need not increase as dramatically. In particular, the ratio of a single slit area to total meshed area (in a two-dimensional projection) is $\delta t\Big/\left(L(r_w - t)\right) \sim \mathcal{O}\left(10^{-9}\right)$, whereas the respective ratio for the number of elements is $\mathcal{O}\left(10^{-4}\right)$. Thus the acceleration zones were sufficiently finely meshed. The quality of the mesh is further evidenced by the almost doubled number of elements (system and well) in the $n \longmapsto 2n$ modification: the presence of additional mixing loci requires a proportionate mesh refinement to capture the turbulent flow structures correctly. In all configurations the error of mass flowrate at outlet relative to expected total generation improved by one order of magnitude between the base and fine meshes.

parameter	symbol	value
dynamic viscosity	μ	$1.4 \times 10^{-5}\mathrm{Pa} \cdot \mathrm{s}$
gas constant	R	$287\mathrm{J}/(\mathrm{kg} \cdot \mathrm{K})$
pipe radius	r_p	$0.0762\mathrm{m}\ (3")$
outer gravel radius	r_g	1m
outer waste radius	r_w	10m
pipe wall thickness	t	$0.00711\mathrm{m}\ (0.28")$
pipe wall roughness	ε *	$1.5 \times 10^{-6}\mathrm{m}$
well length	L	420m
hole radius	r_h	$0.00635\mathrm{m}\ (0.25")$
no. of holes per section	n_h	6
no. of pipe segments	n	28
temperature	T	$15^o\mathrm{C}$
atmospheric pressure	p_{atm}	101325Pa
outlet pressure	p_{o}	100800Pa
generation rate	C	$10^{-6}\mathrm{kg}/(\mathrm{m}^3 \cdot \mathrm{s})$
gravel permeability	k_g †	$3.2 \times 10^{-5}\mathrm{m}^2$
waste permeability	k_w ‡	$1.5 \times 10^{-8}\mathrm{m}^2$

* Typical value for PVC pipes used in landfill well construction, also listed for drawn tubing in the COMSOL manual (COMSOL, 2021, table 3-5, pp 213).

† The gravel lamina's purpose is to support the pipe whilst offering minimal resistance to flow. Thus its permeability is usually several orders of magnitude higher than that of the waste.

‡ This value is characteristic of compacted household waste in medium size municipal landfills.

Table 1: base parameters

configuration	grid	N_{elm}			$\dot{m}_0/\dot{m}_{\mathrm{gen}} - 1$
		system	well	slit area	
(δ, n)					
	base	473293	220203	106	$\mathcal{O}(10^{-11})$
	fine	518797	283594	196	$\mathcal{O}(10^{-12})$
$(2\delta, n)$					
	base	350632	143516	64	$\mathcal{O}(10^{-12})$
	fine	501010	267753	208	$\mathcal{O}(10^{-13})$
$(\delta, 2n)$					
	base	872643	431328	106	$\mathcal{O}(10^{-11})$
	fine	926356	521062	196	$\mathcal{O}(10^{-12})$

Table 2: number of elements N_{elm} used in computational meshes: entire system, well domain (including all slits) and a single slit; and mass flowrate error at outlet relative to total generation

A direct evidence of adequate mesh convergence is given in figure 3 for the basic (δ, n) configuration: the pressure profiles near the interface between the Darcy and continuum flow domains match adequately for the base and fine meshes. The influence on global variables such as radial and longitudinal pressure profiles in the landfill mass away from the acceleration zone as well as variation

within the well was insignificant. The maximal discrepancy between the curves on figure 3 is 3Pa. Since this study aims to seek qualitative insight into the coupling of porous media and continuum flows, and the global impact of turbulence engendered by ingress and mixing, a global precision of 5Pa (maximal difference between solutions on base and fine meshes and 1% out of total head loss) was deemed sufficient for all computations.

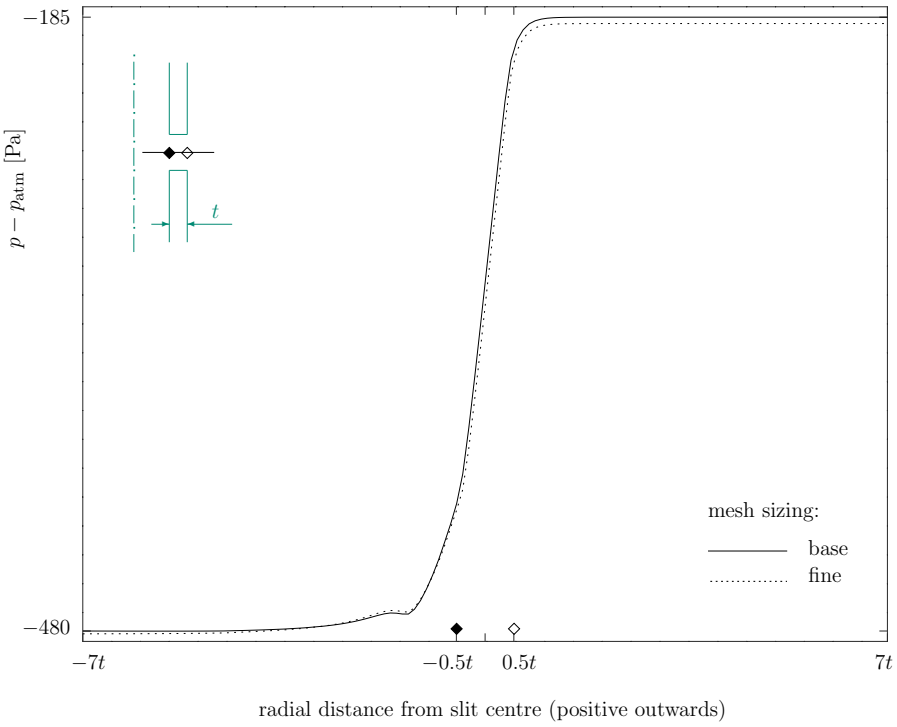

Figure 3: Pressure relative to the atmosphere along centre line of slit 1; inset shows profile path (black, dimensions not to scale)

Hereunder the comparison of two turbulence closure methods is the mainstay of overall model validation. The disparate implementation of the $k - \epsilon$ and $k - \omega$ methods notwithstanding, the numerical results presented in §3 are either visually indistinguishable or exhibit very small quantitative differences in all flow variables.

3 Turbulence impact

From the vantage point of flow modelling as well as flow optimisation in practice, one must look at three parts of this system: pressure distribution within the well, head loss as the fluid moves radially from the porous medium into the pipe, and longitudinal pressure variation in the landfill at a fixed distance from the pipe wall. Whilst it is obvious that system length radial or longitudinal profiles are global entities, the extent to which the localised changes near an aperture affect the entire system is non-trivial. The crux to a correct quantitative representation of the system as a whole lies in the extreme smallness of the well intake area relative to the dimensions of the landfill segment drained. Fathoming where and by what mechanism the applied suction is dissipated, will enable educated decision making as regards the design of new landfills and operation of existing ones. Hereinafter

the interconnection between the aforementioned three flow locales as given by the semi-analytical and fully turbulent models is discussed, beginning with the case of a horizontal well.

Figure 4 exemplifies the behaviour of the velocity vector near the ingress. The radial component increases rapidly as the fluid approaches the slit and decays just as quickly within the pipe. Excluding mixing head losses, the energy is converted into longitudinal velocity. Both curves' gradients indicate the mixing zone width is only a few multiples of the pipe wall thickness t. In medium sized landfills this corresponds to the order of magnitude of $\mathcal{O}\left(10^{-2}\right)$ and $\mathcal{O}\left(10^{-4}\right)$ relative to pipe and landfill radii respectively. These scales attest to the smallness of the zone, to which significant changes in pressure and velocity of the fluid are confined, and allow to infer that the main behaviour near the ingress is of an inner layer type.

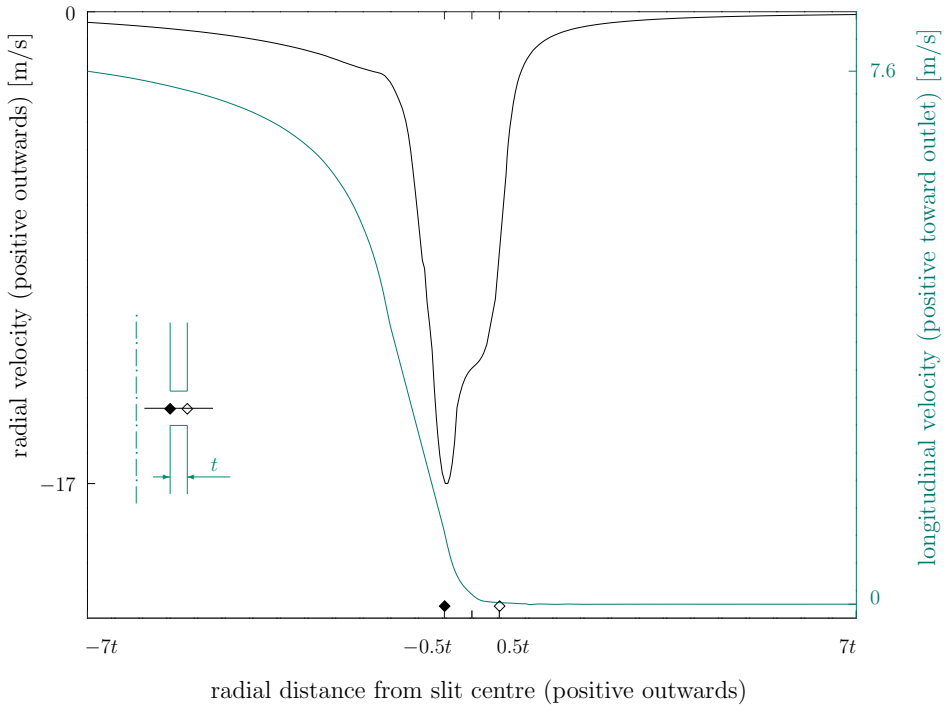

Figure 4: Velocity components along centre line of slit 1; inset showing profile path (black, dimensions not to scale)

Figure 5 illustrates the cumulative effect of these abrupt localised changes: the overall head loss entailed by both turbulence closure models is significantly smaller than the prediction of the semi-analytical solution. As a result, a lesser suction strength would suffice to maintain a sub-atmospheric pressure throughout the system, ergo the power required for an adequate gas extraction is impacted if ingress effects are considered. Since the only other major energy dissipation mechanism in the horizontal well is friction, quantitatively close friction factor profiles within the well prove the ingress turbulence must be the sole source of discrepancy. Figure 6 compares f as computed by (5b) with the Reynolds number expressed via the mass flowrate in the well as $\mathrm{Re} = 2\dot{m}/(\pi\mu r_p)$ for the semi-analytical solution and both turbulence closure models. The agreement between the fully turbulent models is excellent, confirming adequate grid convergence given that the Reynolds number is a derived quantity. Hereinafter, wheresoever results of the two models were visually indistinguishable, only one curve is shown.

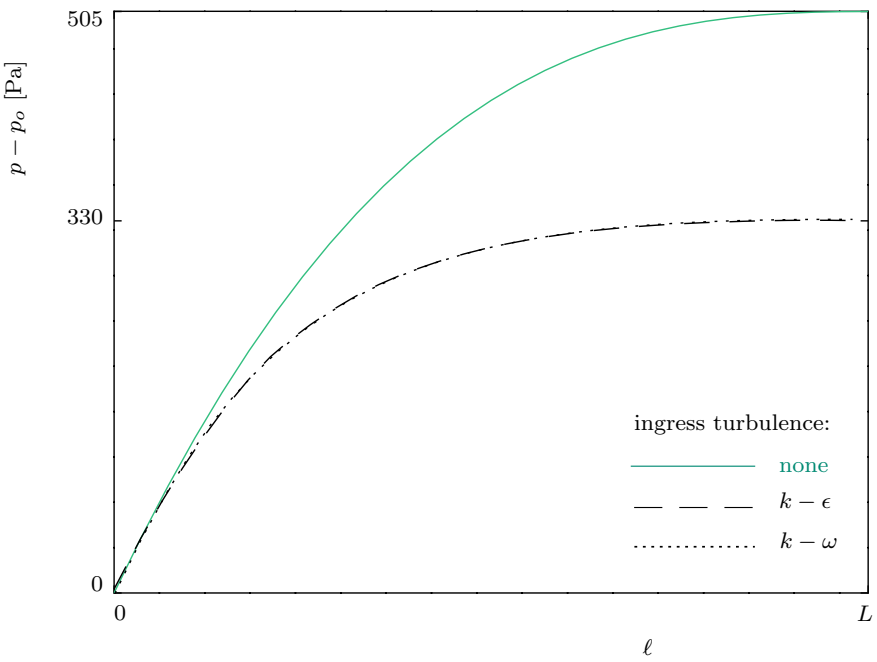

Figure 5: Pressure variation along well centre line (relative to outlet)

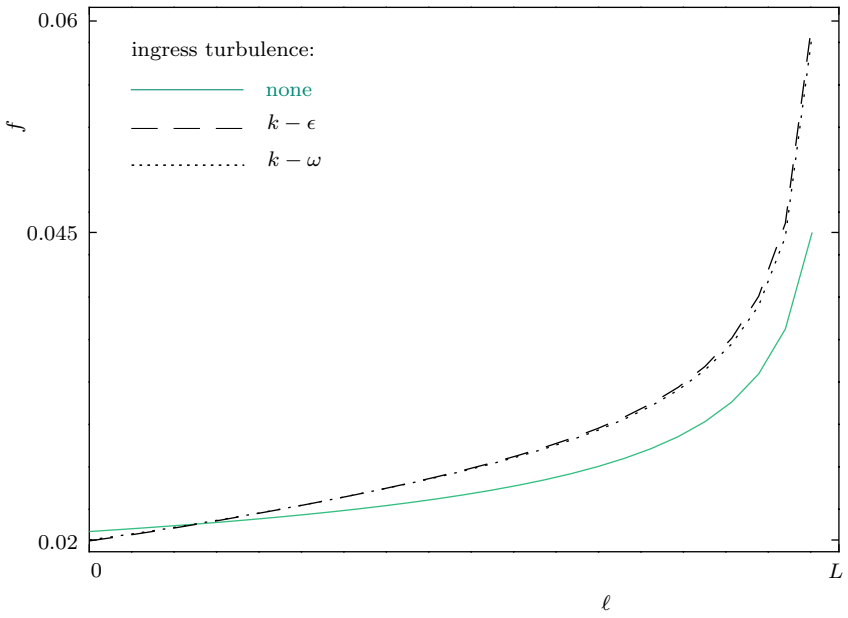

Figure 6: Friction factor variation along well centre line

On the porous medium side of the coupling interface the abrupt radial acceleration toward the ingress aperture induces a step-like decrease in pressure. This effect is progressively more pronounced when moving from the blocked end of the well to the outlet, where the pressure is the lowest. Figure 3 depicts a typical example at the slit closest thereto ($i = 1$): the magnitude of head loss due to ingress and mixing is comparable with the overall head loss due to friction within the pipe (figure 5). The pressure becomes virtually constant at a radial distance of only $2t$ from the slit centre, belying the semi-analytical formulation. That framework's limitation stems from the quasi-1D reduction, based on slow variation in the longitudinal direction inferred via dimensional analysis of the system geometry and overlooking the extreme localised changes taking place near the ingress apertures. A concomitant artefact is the continuity of pressure immediately inside and outside of the pipe wall along the entire length of the well. The current investigation corrected this issue, whereby (4b) is implemented at a discrete set of intervals separated by segments of solid pipe wall, where a no flux (outside) or no slip (inside) condition is imposed instead (figure 2). The resistance of a porous medium to flow is enormous compared to a continuum flow. When the two are coupled, a global minimisation of energy dissipation dictates that most head losses occur in or near the latter part of the system, i.e. at the ingress apertures and within the well. When the curve in figure 3 is continued away from the slit ($r \gg t$), the pressure is not constant, but the gradient is extremely small in comparison to the jump observed near the ingress.

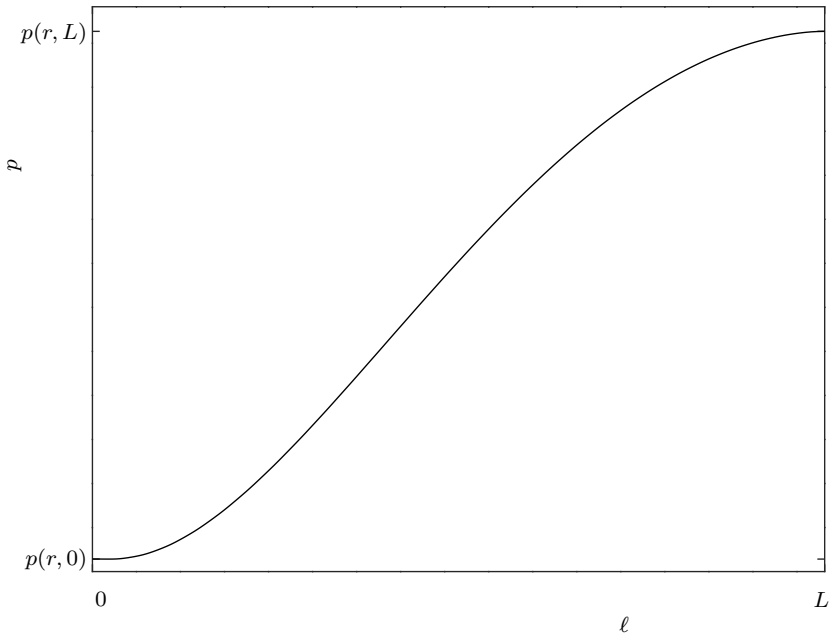

Figure 7: Pressure along cylinder surface of fixed $r \gtrapprox r_p + 2t$

Figure 7 shows a typical pressure profile along any horizontal cylindrical surface at a fixed radius away from the ingress region. The overall change in pressure is on the order of magnitude of a few Pa at the radial distance of $2t$ from the pipe wall or farther. To wit, as long as the permeabilities remain moderate, the global impact of the inner layer created near the ingress apertures amounts to residual velocity and pressure gradient within most of the porous domain. In the field their small magnitude translates into an inability to measure them consistently, if at all. This magnitude correlates strongly with the matrix permeability, mainly that of the waste layer as the largest component of the landfill

system. Figure 8 depicts the total head loss for a range of waste permeabilities on both sides of the nominal value of k_w (table 1) along a radial path beginning outside the ingress inner layer (distance of $7t$ from slit centre) and traversing the landfill to its boundary. Under an adequate operating regime (1–2 orders of magnitude around the clear diamond) the apparent stagnation away from the inner layer implied in figure 3 is no longer counter-intuitive. When one considers the stark difference between resistance to fluid flow posed by a boundary friction only (continuum flow) and a volume filling solid matrix (porous medium flow), it stands to reason that global energy minimisation would favour restricting the head losses to the former. The pressure mounts dramatically at extremely low permeabilities (green / grey part of the graph past the critical point marked by asterisks). Adjusting the vacuum would move the entire system into a sub-atmospheric regime, but the strong gradient would remain. Such permeability ratios and respective suction strength values are not encountered in realistic landfill operation.

In the semi-analytical formulation the head loss due to porous medium resistance erroneously occurs over the waste layer instead of the vicinity of ingress apertures. The prediction of total head loss over the landfill mass is virtually identical to that of the fully turbulent model, but shifted four orders of permeability magnitude: the two lines in figure 8 would coincide if the semi-analytical prediction was moved to the left. This illustrates the principal point this study seeks to establish: accounting for turbulent ingress flow and mixing allows for a global energy minimisation by shifting the locus of primary head dissipation in the landfill from the waste layer to the vicinity of the well.

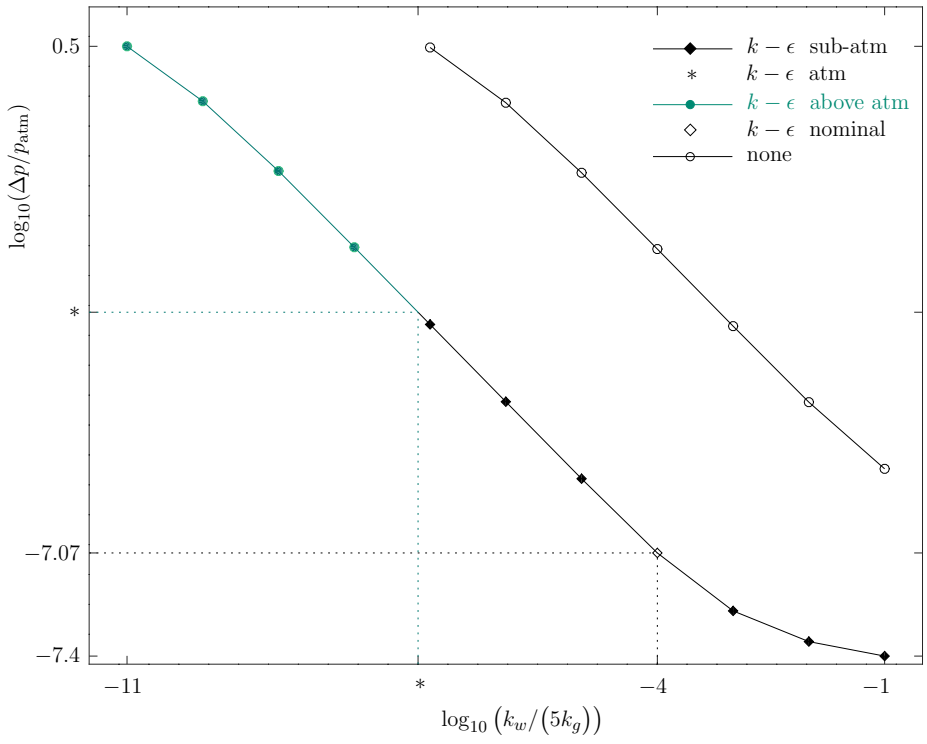

Figure 8: Total head loss across landfill mass along centre line of slit 1 versus permeability ratio on a logarithmic scale: fully turbulent (lower curve) and semi-analytical (upper curve) predictions about the nominal system (clear diamond, table 1)

Another qualitative feature of import shown in figure 7 is the vanishing gradient at the outlet and blocked planes of the system ($\ell = 0$ and $\ell = L$ respectively). By contrast, in the semi-analytical

model the respective profile is of an identical shape to the curve shown in figure 5 with the overall head loss tangibly overestimated, as the abrupt dissipation confined to the inner layer at the coupling interface instead occurs much more slowly over the full volume of the landfill. With the restriction on continuous pressure matching on two sides of the pipe wall relaxed, it was possible to implement a realistic no flux boundary condition on the landfill outlet plane (bar the well outlet itself). As a consequence, the longitudinal variation of the Reynolds number within the well became markedly non-linear. Figure 9 illustrates the discrepancy. With no ingress turbulence the non-linearity of the cumulative mass flowrate or Reynolds number is slight and only visually apparent when examining the incremental inflow quantities (cf. panels (b) and (c) in figures 2–6 of Nec and Huculak (2019)).

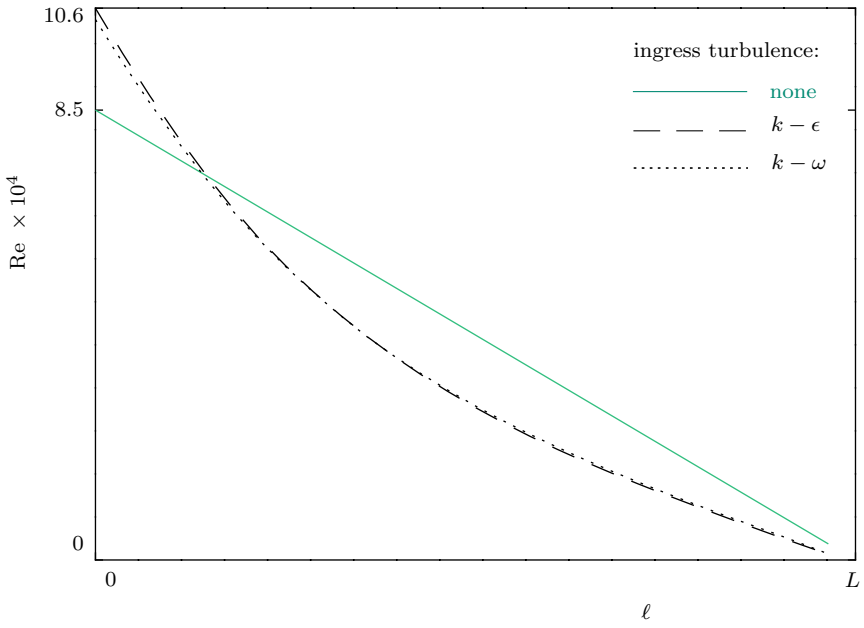

Figure 9: Reynolds number variation along well centre line

In a vertical well a strong localisation of head loss in the vicinity of the ingress along with negligible dissipation over the landfill mass is similarly observed. Figure 10 shows a typical inner layer pressure profile as the fluid enters the aperture, reconstructing the same qualitative features as in figure 3. In this case, however, the jump height is small relative to the overall head loss along a vertically oriented cylindrical surface, cf. figure 11. This happens because the main head loss mechanism is gravity rather than friction, acting equally on the fluid inside and outside of the well. Figure 11 shows that the head loss along any vertical line away from rigid boundaries matches the exponential hydrostatic pressure column given by (5c) with $\dot{m}_i = 0$ and visually appears linear due to the short length of the vertical well. Owing to the dense distribution of apertures in this type of well, the pressure loss between successive perforated sections is small, i.e. $p^2|_{\ell_i} \approx p^2|_{\ell_{i+1}}$, which is equivalent to setting $\dot{m}_i \approx 0$. Thus in a vertical well the inclusion of ingress turbulence corrects the qualitative behaviour of the local pressure field near the ingress, however the impact on the required extraction energy is negligible.

Whilst the quasi-1D approach might serve as a simple initial design tool, this study conclusively shows the importance of including turbulence at the ingress in order to obtain correct local flow velocities in the well-landfill coupled system and a realistic head loss profile over the landfill mass.

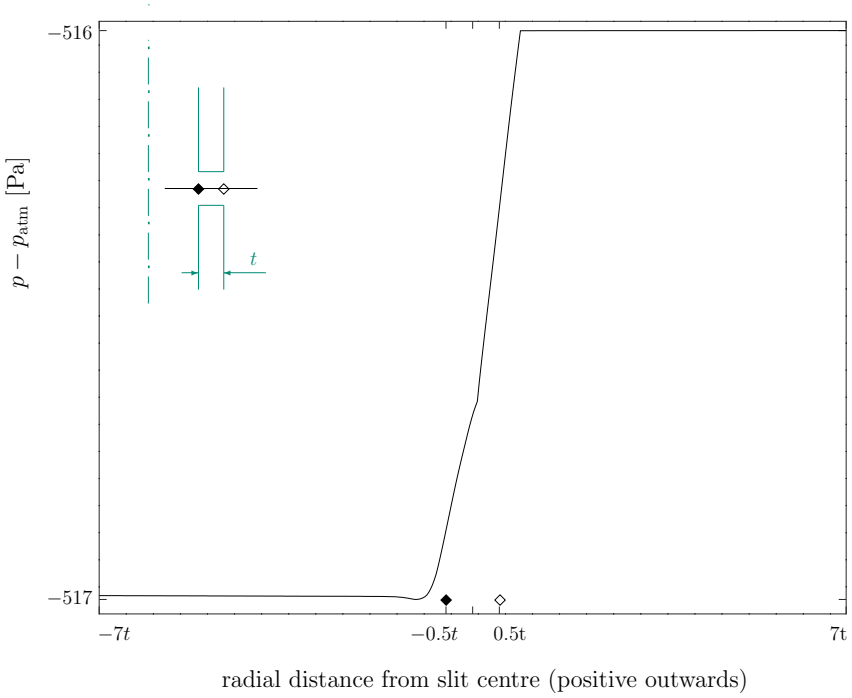

Figure 10: Pressure relative to the atmosphere along centre line of slit 1 in a vertical well of length $L = 20$; inset shows profile path (black, dimensions not to scale)

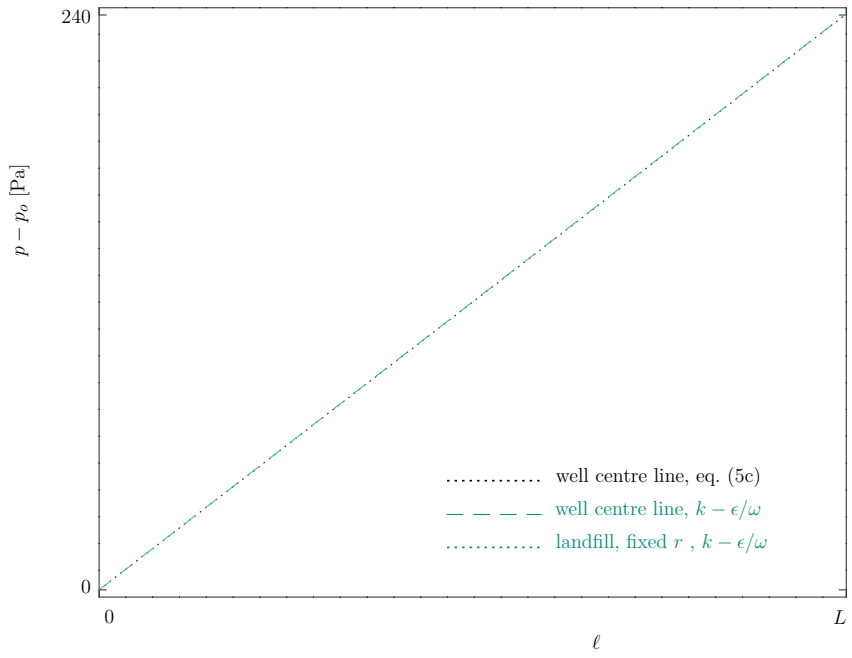

Figure 11: Pressure variation in a vertical well of length $L = 20$ (relative to outlet)

4 Optimisation considerations

Numerical evidence presented heretofore for a horizontal well clearly illustrates that the effective resistance to fluid collection posed by ingress apertures is on par with friction that is widely considered the main mechanism of energy dissipation in this system. This brings to the fore the question of optimising such design parameters as the aperture size and frequency of perforated sections for a minimal total head loss. In Nec and Huculak (2019) it was conjectured these geometric parameters might provide an alternative flow control strategy, when high boundary resistance (infinite when the boundary is sealed) begets an irresponsiveness to the outlet vacuum. Since it was established herein that dissipation within the landfill is very small, it stands to reason the optimisation might be focussed on the well and its immediate surroundings. Given that the quasi-1D formulation misrepresents the locus of head loss within the landfill, it is not equipped to answer the question of an optimal geometric design adequately. Albeit the full optimisation problem is beyond the ambit of the current framework, this section aims to touch upon the points expected to underpin its solution.

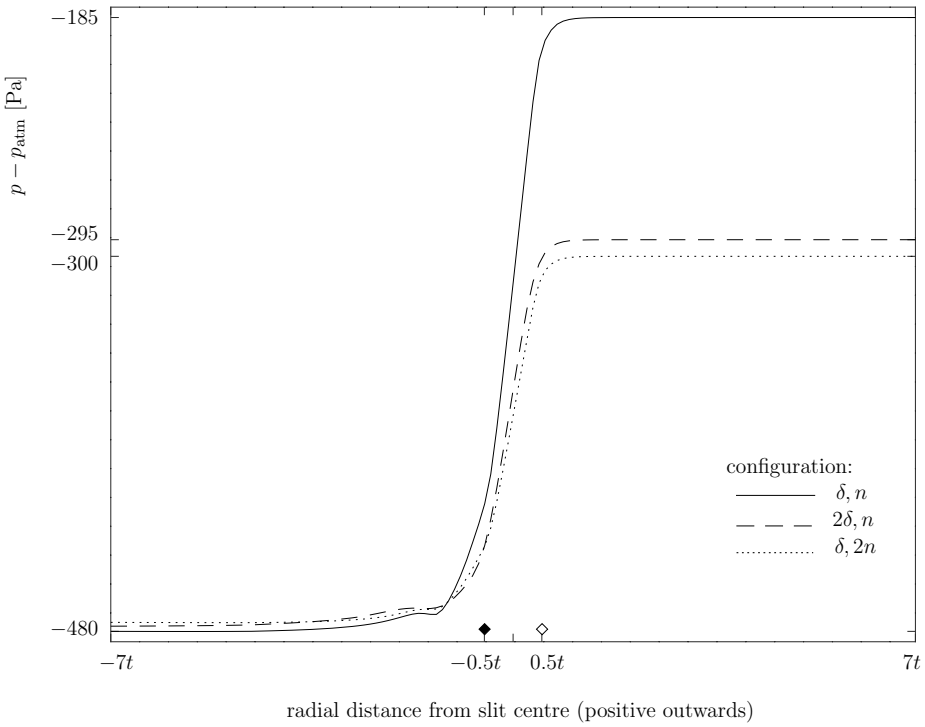

Figure 12: Pressure relative to the atmosphere along centre line of first coincident set of slits: geometry impact; see inset of figure 3 for profile path

The basic geometry changes tested were doubling the slit width $\delta \longmapsto 2\delta$ (equivalent to $n_h \longmapsto 2n_h$ or $r_h \longmapsto \sqrt{2}r_h$) or number of segments $n \longmapsto 2n$. Both modified configurations have identical total intake area, and it is possible to compare aperture traversing profiles at matching longitudinal positions as slit locations coincide at every other index i. The first question is how the amplitude of the step-like change in pressure during the passage through the slit is affected. Figure 12 shows the pressure profiles at the first coincident set of slits. As might be expected, albeit doubling the intake area diminishes the pressure jump, the reduction factor equals approximately 1.6. A much less trivial observation is that both modified configurations entail a virtually identical head loss.

The quasi-1D solution predicted a similar outcome for a partly permeable boundary (figure 6 of Nec and Huculak (2019)), but is unsuitable for the analysis of sealed domains. The functional shape of p in (3) with zero flux on the outer boundary implies that the mass of fluid $\Delta\dot{m}_i$ inflowing into the i-th slit is independent of its width:

$$\Delta\dot{m}_i = \pi r_p \delta \, \frac{k_g}{\mu R T} \frac{\mathrm{d}p^2}{\mathrm{d}r} = \pi\delta \, \frac{k_g a_g}{\mu R T}, \tag{9a}$$

where a_g is the integration constant a in (3) for the gravel lamina (the generation rate vanishes therein), obtained by continuity of pressure and velocity with the waste layer:

$$a_g = \frac{\mu R T C}{k_g} \left(r_w^2 - r_g^2\right). \tag{9b}$$

Further technical detail is available in appendix B of Nec and Huculak (2019), equation (B3). Combining (9a) and (9b) yields

$$\Delta\dot{m}_i = \pi\delta \, C \left(r_w^2 - r_g^2\right). \tag{9c}$$

By construction, the quasi-1D model requires each landfill segment to be condensed into a thin disc aligned with the respective slit by mapping $C \longmapsto C/\delta$. Thus the product $\delta\, C$ is fixed regardless of the slit width chosen. As a result only adjusting the number of perforated sections n will result in a distinct solution owing to the non-linearity of (5a).

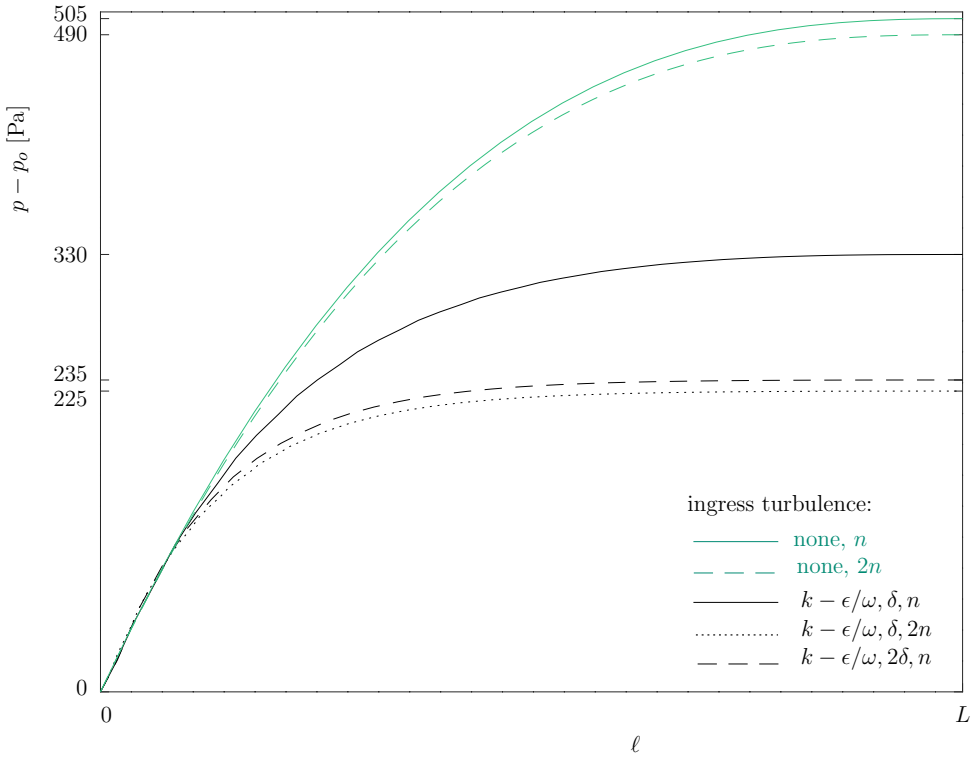

Figure 13: Pressure variation along well centre line (relative to outlet): geometry impact

Figure 13 shows the pressure profiles within the well for all germane configurations for the fully turbulent and quasi-1D models. In the former case a doubled intake area resulted in a head loss

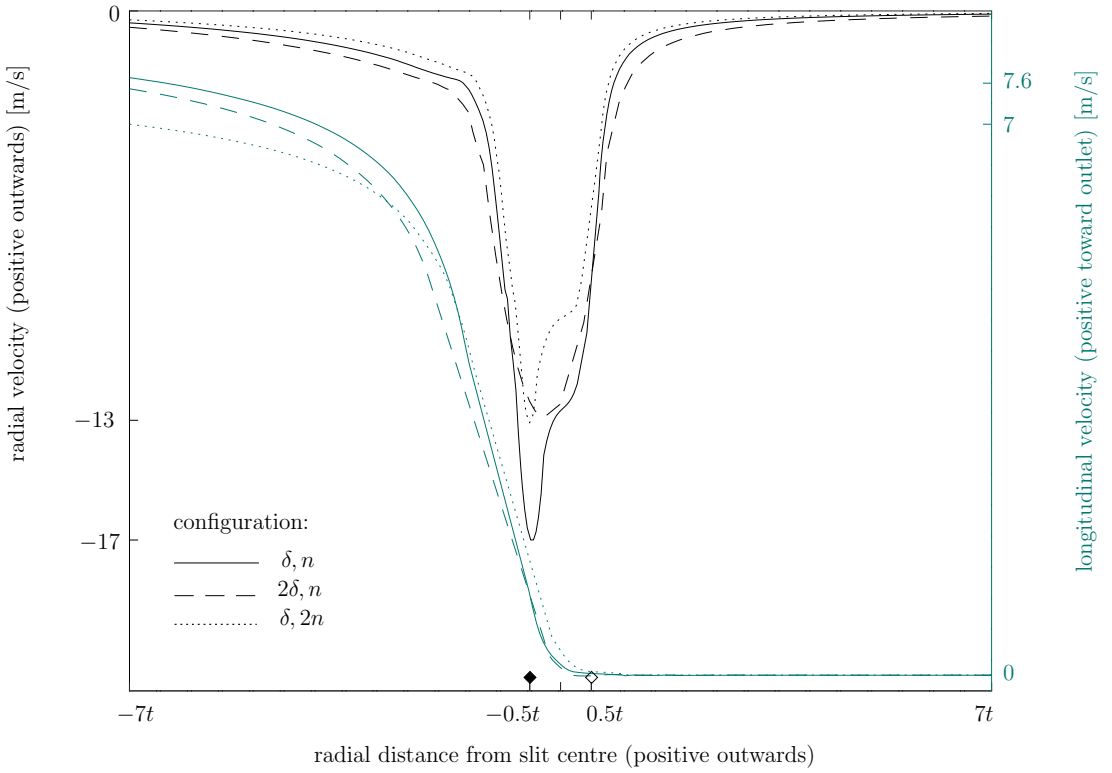

Figure 14: Velocity components along centre line of first coincident set of slits: geometry impact; see inset of figure 3 for profile path

reduction similar to that demonstrated in figure 12. It is therefore conjectured that both geometric modifications are equivalent for all practical purposes. Without ingress turbulence doubling the perforation frequency is only reflected in a minor deviation due to fluid compressibility.

Judging solely by the pressure profiles, one might infer a monotonic dependence, whereby it is always beneficial to increase the intake area. A scrutiny of the ingress velocity profiles evinces reasons for caution. Comparing the radial velocity components in figure 14, it is seen that both modifications incur a reduction of the maximal velocity (in absolute value) by a factor of approximately 1.3. The modification $n \longmapsto 2n$ retains the same profile shape as the (δ, n) configuration, but with lesser acceleration (solid and dotted black curves). In the $\delta \longmapsto 2\delta$ modification the incoming fluid develops the same radial velocity as with $n \longmapsto 2n$, but the doubled physical dimension of the aperture allows for a slightly wider inner layer. The respective maximal longitudinal velocity changes are not great, yet the flow inside the well is faster for the $(2\delta,\ n)$ configuration. An interesting optimisation problem emerges: it is possible to modify the aperture radius continuously, whereas the number of perforated sections is a discrete variable. In light of the above, there should be an optimal configuration with (δ_*, n_*), where energy dissipation due to mixing at the perforated sections is minimal.

5 Discussion

Landfills have been constructed and operated for many decades without an adequate understanding of the porous medium - continuum flow coupled system and as a result with only intermittent success as regards collection control. The salient physical property governing the flow is the overall effective resistance of the porous matrix to flow, also known as permeability and often misconstrued to be an intrinsic and thus objectively quantifiable property of the porous matrix alone. In reality this property is strongly affected by boundaries (sealed or partly permeable). Instances of misjudging this quantity have resulted in the loss of flow control, e.g. a sealed boundary presents a locally infinite resistance with the global effect of flowrate irresponsiveness to suction strength (Nec and Huculak, 2019). The incorporation of ingress turbulence evinces a new and potentially no less significant source of effective resistance: a highly localised inner layer near each intake aperture, responsible for the dissipation of most of the head available at the respective position within the well. In the case of horizontal wells with sparse perforated sections the second head loss mechanism is friction. Excluding ingress turbulence effects leads to an erroneous representation of the loci of the highest pressure and its gradient in the system as well as an overestimation of the required extraction energy. By contrast, in a vertical well the perforation frequency is higher, since refuse weight and compacting machinery pose less risk to the structural integrity of the pipe. The dominant head loss mechanism is gravity, which affects the fluid uniformly inside and outside the well. Thus if one is interested in the estimate of total extraction energy, but not the pressure distribution within the landfill or mixing flow structures at the perforations, modelling turbulence near the ingress is not as important.

In a correctly functioning landfill facility the pressure throughout the system is sub-atmospheric in order to avoid a hazardous accumulation of a flammable and explosive gas. Ideally the highest pressure is just below atmospheric to minimise collection energy. When the generation rate is high, it is the operators' responsibility to increase the suction vacuum to maintain sub-atmospheric pressure. The modelling presented in this study pertains solely to such a sustainable operational regime.

Insight as to the location of the highest pressure in the system is the crux of engineering design and operation of landfill facilities. The application is inherently plagued by uncertainties associated with estimating gas generation rate and waste permeability over time. In most countries direct monitoring of pressure is mandated, but is usually kept to a minimum due to the cost of equipment installation and maintenance. The measurements are used as a binary indicator of the pressure being sub-atmospheric or exceeding atmospheric in order to adjust the suction vacuum. Such data commonly remain unpublished for a fourfold reason: extreme difficulty to obtain consistent measurements under controlled conditions due to barometric fluctuations, water table shifts and ongoing site work; uniqueness of waste content and gas collection network at each landfill site; invalidation of the measurements in time as the waste degradation progresses; and the deemed baffling experience that the pressure is virtually constant away from the well (within the precision of commonly available equipment). In this regard the flow field around gas wells is dissimilar from that of hydraulic wells, where head losses are known (consistently measured) to be much more gradual due to the fluid's almost a thousandfold higher density. The porous medium flow is coupled to the unobstructed flow in the well with velocity near the ingress surging several orders of magnitude. From the vantage point of physics, the resistance posed by the porous matrix to the passage of fluid by far exceeds that of continuum flow: the least overall energy dissipation occurs when the velocity and thus pressure gradient are extremely small in the porous medium, and most of the acceleration takes place at the interface with the continuum flow. The simplistic one-dimensional model (3) predicts this phenomenon to some extent when more than three orders of magnitude separate the permeabilities of the contiguous gravel and waste layers. Nonetheless, the gradual head loss over the gravel lamina predicted by (3) defies field experience. Including turbulence effects at the ingress to the well resolves this issue and in fact provides a picture that comes the closest to explaining the dearth of success in measuring tangible head losses anywhere in the porous matrix.

The Darcy friction factor f as given by the Colebrook equation (5b) accounts for turbulence engendered by the roughness of the pipe's inner wall. Only a fully turbulent model can capture

the losses due to ingress and mixing with the crossflow. Most of the head available within the well at each perforated section dissipates within a few multiples of the wall thickness t outside of the ingress aperture. The global impact of this locally turbulent flow on the radial pressure profile away from the ingress amounts to the residual velocity and pressure gradient as the fluid traverses the porous matrix from the outer circumference of the landfill toward the well. Both are small, but not zero: mathematically the radial velocity and pressure gradient vanish only on the landfill perimeter. Denote the pressure outside of the acceleration zone near ingress aperture i by $p(7t, \ell_i)$, and for simplicity take the pressure at the landfill perimeter equal to the atmospheric pressure p_{atm}. The radial gradient over the landfill mass at ℓ_i will then roughly equal $\big(p_{\text{atm}} - p(7t, \ell_i)\big)/r_w$, where the landfill radius r_w is much larger than the pipe radius r_p or its wall thickness t. With adequate suction the difference $p_{\text{atm}} - p(7t, \ell_i)$ is on the order of a few tens of Pa when $k_g/k_w \sim \mathcal{O}\big(10^7\big)$ and reduces to nought when $k_g/k_w \sim \mathcal{O}\big(10^4\big)$ or lower, whereas r_w is about 10m, often more. Thus the residual gradient is no more than a few Pa even in cases of extreme permeability disparity. When the head $p_{\text{atm}} - p(7t, \ell_i)$ varies with geometric or physical parameters, the resulting residual pressure gradient over the porous laminae will change accordingly, whilst remaining small relative to the overall head loss along the entire length of the well. Thus somewhat counter-intuitively the pressure variation and hence fluid velocity in the landfill always remain minimal. For this reason modelling turbulence within either of the porous laminae is unnecessary. In fact, even Brinkman's correction that uses a non-linear velocity term to amend Darcy's law at higher velocities, was not required.

When the mass flowrate controllability via the outlet vacuum diminishes, one of the alternative control mechanisms suggested is increasing the perforation frequency (Nec and Huculak, 2019). The current results imply that strategy might improve the overall head loss in the well up to a certain point, but thenceforward adding more apertures will incur higher losses, since each entry point corresponds to a stream of fluid that must mix and adjust its flow direction. An unconventional optimisation problem arises, where one might vary the aperture size, a continuous parameter, but a decision to add or remove a perforated section begets a discontinuous jump in the overall head loss.

The landfill well is a more complicated system than either jet injection or pipe juncture, although in both cases a stream of fluid mixes with a crossflow. An attempt at adaptation of existing empirical head loss models for these classical systems to the landfill well did not bear fruit. The crucial distinctive features of the well are an uncontrolled angle of entry at the interface of two disparate flow regimes, and the multiplicity of apertures with the crossflow Reynolds number varying from zero at the blocked end to $\mathcal{O}\left(10^4\right)$ at the outlet. A suitable analytical description via localised asymptotics of the inner layer based on the current computational fluid dynamics results is a topic of future study.

Acknowledgements

Field data and landfill design parameters furnished by GNH Consulting Ltd., Delta, British Columbia, Canada, are gratefully acknowledged. YN acknowledges the support of Canada Foundation for Innovation grant # 35174, and Natural Sciences and Engineering Research Council of Canada grant # 2017-04985.

References

Broadwell JE, Breidenthal RE (1984) Structure and mixing of a transverse jet in incompressible flow. J Fluid Mech 148:405–412

Carman PC (1937) Fluid flow through granular beds. Trans Inst Chem Eng 15:150–167

Colebrook CF (1939) Turbulent flow in pipes, with particular reference to the transition region between the smooth and rough pipe laws. J Inst Civil Eng 11:133–156

COMSOL (2021) CFD Module User's Guide. COMSOL Multiphysics, v. 6.0

Feng SJ, Zheng QT, Xie HJ (2015) A model for gas pressure in layered landfills with horizontal gas collection systems. Comput Geotech 68:117–127

Fulks WB, Guenther RB, Roetman EL (1971) Equations of motion and continuity for fluid flow in a porous medium. Acta Mech 12:121–129

Halvorsen D, Nec Y, Huculak G (2019) Horizontal landfill gas wells: geometry, physics of flow and connection with the atmosphere. Phys Chem Earth 113:50–62

Henderson N, Brêttas JC, Sacco WF (2010) A three-parameter Kozeny-Carman generalized equation for fractal porous media. Chem Eng Sci 65:4432–4442

Hu J, Ke H, Lan JW, Chen YM, Meng M (2020) A dual-porosity model for coupled leachate and gas flow to vertical wells in municipal solid waste landfills. Géotechnique 70:406–420

Idel'chik IE (1966) Handbook of hydraulic resistance: coefficients of local resistance and of friction. ERDA Div. Phys. Res

Ke H, Hu J, Chen YM, Lan JW, Zhan LT, Meng M, Yang YQ, Li YC (2021) Foam-induced high gas pressures in wet municipal solid waste landfills. Géotechnique 0:in press

Lu SF, Feng SJ, Zheng QT, Bai ZB (2021) A multi-phase, multi-component model for coupled processes in anaerobic landfills: theory, implementation and validation. Géotechnique 71:826–842

Nec Y, Huculak G (2017) Solution of weakly compressible isothermal flow in landfill gas collection networks. Fluid Dyn Res 49:065505

Nec Y, Huculak G (2019) Landfill gas flow: collection by horizontal wells. Transp Porous Media 130:769–797

Octave (2020) GNU, v. 6.1.0

Panda MN, Lake LW (1994) Estimation of single-phase permeability from parameters of particle-size distribution. Am Assoc Pet Geol Bull 78(7):1028–1039

Rees-White TC, Mønster J, Beaven RP, Scheutz C (2019) Measuring methane emissions from a UK landfill using the tracer dispersion method and the influence of operational and environmental factors. Waste Manage 87:870–882

Whitaker S (1986) Flow in porous media I: A theoretical derivation of Darcy's law. Transp Porous Media 1:3–25

White FM (1999) Fluid Mechanics. McGraw Hill, 4th edition

Wise WR, Townsend TG (2011) One-dimensional gas flow models for municipal solid waste landfills: cylindrical and spherical symmetries. J Environ Eng 137:514–516